Flow Normal to a Flat Plate of a Viscoplastic Fluid with Inertia Effects

Frédéric Savreux, Pascal Jay, and Albert Magnin
Laboratoire de Rhéologie, Université de Grenoble (UJF, INPG) et CNRS (UMR 5520), 38041 Grenoble Cedex 9, France

DOI 10.1002/aic.10488
Published online in Wiley InterScience (www.interscience.wiley.com).

The two-dimensional (2-D) flow normal to a flat plate of a Bingham fluid is studied numerically. The effects of plasticity and inertia are investigated. The detailed structure of the flow is examined in relation to a large range of the Oldroyd number ($0 \leq Od \leq 100$) and of the Reynolds number ($0 \leq Re \leq 10$). The strong influence of these parameters, especially on the rigid zones and on the vortex zone, is shown. The drag coefficient is also calculated and some analytic relationships are proposed. The results are compared with the few other data available. © 2005 American Institute of Chemical Engineers *AIChE J,* 51: 750–758, 2005

Keywords: viscoplastic fluid, drag coefficient, yield stress, plate, inertia

Introduction

Many fluids prepared in chemical engineering—such as gels, slurries, suspensions, and dough—have a viscoplastic behavior. Throughout the manufacturing process, they are stretched, squeezed, stirred, mixed, and, in many situations, the fluid has to flow around different geometric configurations. For example, in a rotational mixing vessel, the fluid is pushed by an impeller, which may consist of cylindrical and/or flat parts. So to optimize a viscoplastic fluid mixer, it is necessary to have a good understanding of the behavior (in terms of flow structure and power consumption) of this type of fluid when it flows around these different bodies and when the effects of inertia and viscoplasticity are significant. The study of flow around a cylinder was previously reported (Deglo de Besses et al., 2003). In this study, the flow past a normal flat plate is considered. Numerous studies, both experimental and numerical, have been carried out on this subject, but especially for Newtonian fluids. Tomotika and Aoi (1952), with a simplified numerical approach based on Oseen's equations of motion, determined the influence of the Reynolds number (for $0 < Re < 5$) on the drag coefficient and calculated the flow patterns formed by two standing eddies behind the plate. Tamada et al. (1983) used the Navier–Stokes equations and determined the variation in drag coefficient for a Reynolds number up to 10. Hudson and Dennis (1985) also solved these equations and determined the streamline patterns for Re up to 20. They compared their numerical results to experimental values obtained by Acrivos et al. (1968). Dennis et al. (1993) proposed a very complete numerical and experimental approach for Re up to 100. To solve the Navier–Stokes equations, they used a finite-difference method and a vorticity–stream function formulation. They compared their results with experimental and numerical values obtained by Ingham et al. (1990). Their geometry is used in the present paper. In et al. (1995) proposed a new numerical scheme to improve the treatment of the tip singularity and they showed the effect of the angle of incidence on both the drag coefficient and streamline patterns.

In the case of viscoplastic fluids, reported studies are more scarce (Chabbra, 1993), and most articles deal with cylinders and spheres (Beris et al., 1985; Liu et al., 2002; Pazwash and Robertson, 1975; Zisis and Mitsoulis, 2002). For flat plates parallel to flow, Piau (2002) shows a new approach for characterizing the viscoplastic boundary layer. For normal plate flow in an infinite medium, the only works seem to be those of Brookes and Whitmore (1968, 1969). After an experimental investigation using a Bingham fluid, they show the influence of the area of the plate on the static drag and propose an analytical relation given the static drag force vs. the projected area and the yield stress. Unfortunately, however, the papers are not detailed enough to be entirely useful.

When a viscoplastic fluid flows past a static body, some rigid

Correspondence concerning this article should be addressed to P. Jay at pascal.jay@ujf-grenoble.fr.

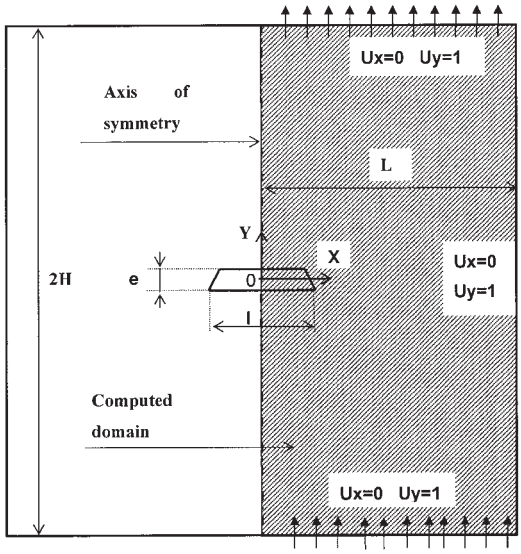

Figure 1. Computational domain and boundary conditions.

zones occur. In cosmetics or in food processing industries these zones, and particularly the static ones, must be eliminated because of bacterial development. Theses zones depend on both the geometry and the dimensionless Reynolds (Re), Oldroyd (Od), and shear-thinning index numbers. Therefore, to improve the quality of this type of product, it is very important to have a good idea of the changes occurring in these zones as a function of these parameters. Their influence on the recirculation zones must also be well defined. Moreover, the design of experimental or industrial setups needs to take into account power consumption. The goal of this work is thus to obtain a better knowledge of these different points by using a numerical approach.

This article is organized into three sections. In the first section, the numerical modeling is described in detail along with the boundary conditions, the definition of the viscoplastic model and its regularization, the characterization of the rigid zones, and the mesh. The results obtained for Newtonian and Bingham viscoplastic creeping flows are shown in the second section and the effects of inertia are discussed in the third section.

Numerical Modeling

The flow normal to a flat plate of a viscoplastic fluid in isothermal conditions is considered. The medium is assumed to be infinite. The geometric definition and the boundary conditions are shown in Figure 1. The length and breadth of the plate are respectively l and e ($e = 0.15l$), and those of the calculation domain $2H$ and L. The plate is chamfered with an angle of 30°. The velocity is equal to zero on the plate and to U_y on the limits of the domain. There is adherence of the fluid on the plate.

The "Polyflow" finite-element program developed by Fluent Inc. (Lebanon, NH) was used. This code is based on a mixed pressure–velocity formulation. Velocity interpolation in an element is quadratic, whereas pressure interpolation is linear and continuous. Convergence is obtained by a Newton algorithm coupled with Picard iterations (except for the Newtonian case). Iterations end when the maximum variation in relative velocity is $<10^{-5}$. The calculations were run on a Hewlett–Packard PC with 500 MB of RDRAM at 400 MHz and an Intel P4 processor clocked at 1.5 GHz.

The Bingham model and the dimensionless parameters

The Bingham model is commonly used to describe the behavior of yield stress fluids. If τ_0 is the yield stress and K is the consistency coefficient, it can be written as follows

$$\begin{cases} \tau_{ij} = 2\left(K + \dfrac{\tau_0}{\dot{\gamma}}\right) D_{ij} & \text{if } \tau_{II} > \tau_0 \\ D_{ij} = 0 & \text{if } \tau_{II} \le \tau_0 \end{cases} \tag{1}$$

where D_{ij} is the strain rate tensor, defined by

$$D_{ij} = \frac{1}{2}\left(\frac{\partial u_i}{\partial x_j} + \frac{\partial u_j}{\partial x_i}\right) \tag{2}$$

$\dot{\gamma}$ is the second invariant of the strain rate tensor

$$\dot{\gamma} = \sqrt{2 D_{ij} D_{ij}} \tag{3}$$

and τ_{II} is the second invariant of the stress tensor

$$\tau_{II} = \sqrt{(1/2)\tau_{ij}\tau_{ij}} \tag{4}$$

In regions where τ_{II} is below the yield stress τ_0, the fluid exhibits no deformation and a solid structure is formed. These regions are called unyielded or rigid zones. Above τ_0, the flow is sheared and the fluid has a Newtonian behavior.

Dimensionless equations are formed by scaling the length by l (the greater length of the plate), the velocity by U_y, and the pressure and stresses by $K(U_y/l)$. Thus the system is reduced to two dimensionless parameters:

(1) The Oldroyd (Bingham) or yield stress number

$$\mathrm{Od} = \frac{\tau_0}{K\left(\dfrac{U_y}{l}\right)} \tag{5}$$

(2) The viscous Reynolds number

$$\mathrm{Re} = \frac{\rho U_y^2}{K\left(\dfrac{U_y}{l}\right)} \tag{6}$$

The plastic Reynolds number can be expressed as

$$\mathrm{S} = \frac{\mathrm{Re}}{\mathrm{Od}} \tag{7}$$

Regularization of the model

As can be seen from the set of expressions in Eq. 1, the Bingham model shows a discontinuity for $\tau = \tau_0$. To remove

this singularity, different solutions based on the regularization of these equations have been proposed (Burgos and Alexandrou, 1999). However, in numerous papers and in most of the recent ones (for example, Alexandrou et al., 2001; Blackery and Mitsoulis, 2002; Smyrnaios and Tsamopoulos, 2001), the method developed by Papanastasiou (1987) is generally used. Burgos and Alexandrou (1999) showed the accuracy of this approach. This method proposes to introduce an exponential part in the model, which becomes

$$\tau_{ij} = 2\left[1 + \frac{\mathrm{Od}}{\dot{\gamma}}(1 - e^{-m\dot{\gamma}})\right]D_{ij} \tag{8}$$

Therefore, the model becomes continuous, although this regularization includes a parameter m. When m tends toward infinity, this model is equivalent to the initial model. Thus to have sufficient accuracy and results that are independent of m, m must have a relatively high value. This value depends on Od. For small values of Od, m must have a very high value ($m \approx 10^5$). On the other hand, for a larger Od number (Od = 10), m can be relatively small ($m \approx 100$). In this work, the value of this parameter was established after a study of its influence on the flow morphology and on the drag coefficient.

Dimension of the domain and mesh

In this work, the medium is considered to be infinite, so it is necessary to adjust the dimension of the domain (L and H, Figure 1) to verify this hypothesis. In the case of a Newtonian fluid, In et al. (1995) proposed a circular domain of radius equal to 83 times the half length of the plate for a Reynolds number between 0.1 and 30. Thus, for the Newtonian case, a domain of characteristics $L = H = 85l$ (l is the length of the plate Figure 1), was chosen. It has been verified that for a greater domain there is no modification in the drag coefficient. For viscoplastic fluid cases, there are no results in the literature. In this study, two criteria have been used to verify the infinity of the medium. First, the drag force must be independent of L and H above a certain value of these dimensions. Second, in the same way, the size and shape of the unyielded zones must also be independent of these lengths. The optimum size of the domain in fact depends on the dimensionless numbers and particularly on the Oldroyd number. When this parameter is small, the problem is equivalent to a Newtonian one and therefore the size of the domain must be chosen as in In et al (1995). On the other hand, when Od is large, as the size of the shear flow zone becomes very small, the domain can be smaller. So, after very numerous calculations, and by using the two previous criteria, two domains (in addition to the previous one for the Newtonian case) depending on Od were determined: for $0.1 \leq \mathrm{Od} \leq 0.5$, $L = 20l$, $H = 30l$, and for larger Od, $L = H = 12l$. For each case, if the dimensions L or H are increased, changes in both the drag coefficient and the geometry of the unyielded zones are smaller than 10^{-2}.

The mesh used in this study is shown in Figure 2. The influence of the mesh on the results was studied systematically. The rigid dead zones are calculated in this study. For the shape of these zones to be independent of the mesh, it must be very accurate. Therefore, near the plate, the mesh was highly refined. On the other hand, determining the drag coefficient needs

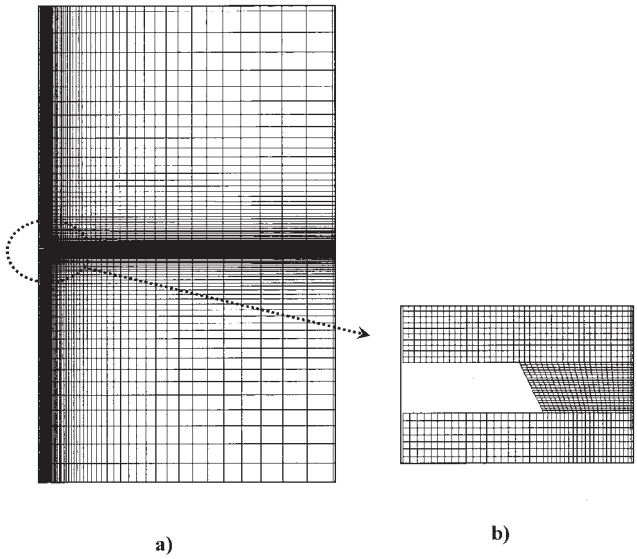

Figure 2. Finite-element mesh used in the simulations: (a) overall mesh; (b) zoom on the plate.

far fewer nodes to be mesh-independent, and thus the rest of the mesh has larger elements, making it possible to maintain a reasonable CPU time. The domains ($L = H = 85l$), ($L = 20l$, $H = 30l$), and ($L = H = 12l$) have, respectively, 13,916, 9972, and 8900 nodes.

CPU time fluctuates typically between 300 s (Od = 0, Re = 0.01) and 18000 seconds (Od = 10, Re = 0.01).

Newtonian Fluids Case

As seen in the first part, there are very few results for viscoplastic fluids. However, some reports have been published for the Newtonian case and these can be used to validate the overall approach to this problem. This is the aim of this section.

Different authors have determined the drag coefficient of a normal plate for a Newtonian fluid and for a plate without thickness: Dennis et al. (1993) in experimental and numerical studies; Tamada et al. (1983) and Tomotika and Aoi (1952) in numerical ones. This drag coefficient is defined by

$$C_d = \frac{2 \times F_y}{\rho U^2 l} \tag{9}$$

where U is the fluid velocity away from the plate, F_y is the drag force, and ρ is the density of fluid.

Figure 3 shows the curve giving the drag coefficient vs. the Reynolds number with results obtained in this present work for $\mathrm{Re} \geq 0.01$, and those of the previous authors. The curves are described by the following equation, which is valid for $0.1 \leq \mathrm{Re} \leq 30$

$$C_d = \frac{1.2732}{\mathrm{Re}} + 1.2549 \times \mathrm{Re}^{-0.34} \tag{10}$$

It can be observed that there is a very good agreement between the results of this study and those obtained by these different authors.

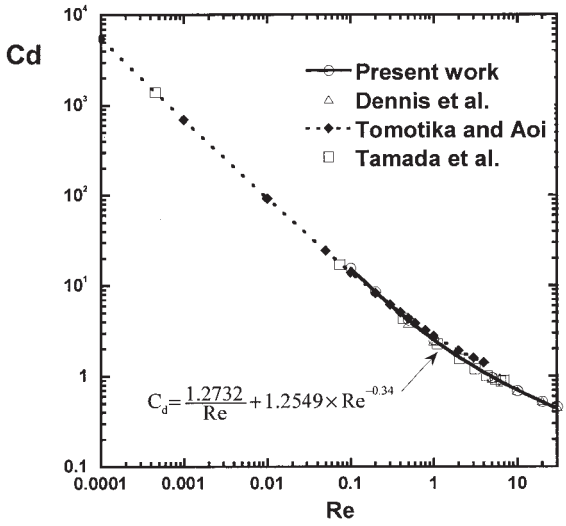

Figure 3. Drag coefficient vs. Reynolds number for a Newtonian fluid (Od = 0).

Viscoplastic Fluids Case

When a viscoplastic fluid flows past a normal plate, four different rigid or unyielded zones (colored in gray in Figure 4) can be observed. The first region (zone 1) surrounds the plate and confines the flow in a limited space. The frontier of this region creates, for the complete domain, a figure of eight

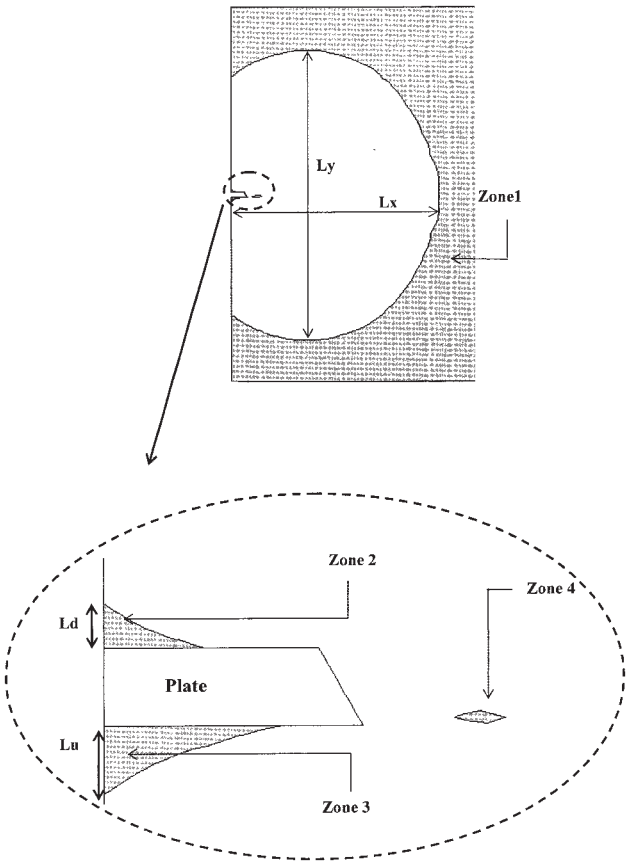

Figure 4. Definition of unyielded or rigid zones.

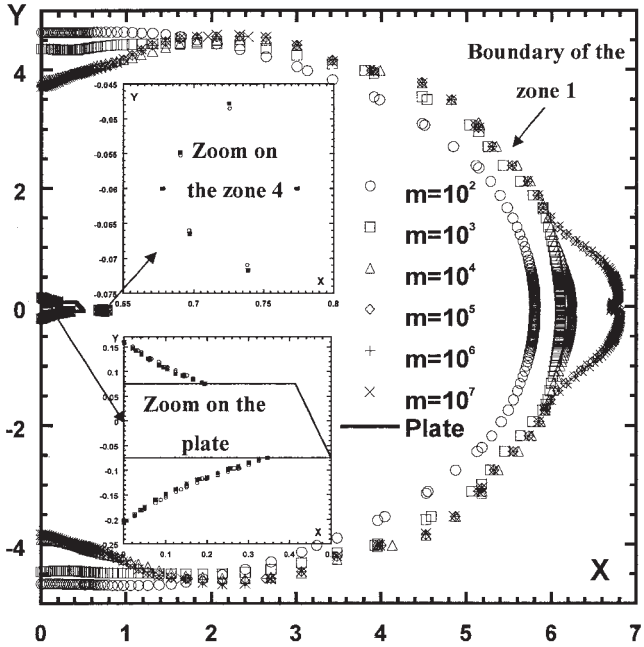

Figure 5. Yielded surfaces calculated for various values of the regularization parameter *m* (Od = 0.5).

centered on the plate. The second region (zones 2 and 3) constitutes rigid static zones (for the existence of theses zones see Beris et al., 1985). They are attached to the plate and their shape is roughly triangular. The last region (zone 4) is a very small and elongated rigid moving zone.

The regularization parameter m has a substantial influence on the size of these different zones (Burgos and Alexandrou, 1999; Liu et al., 2002; Zisis and Mitsoulis, 2002). In this study, a range of m from 10^2 to 10^7 was tested for different Od numbers. Figure 5 shows the influence of m on these regions. From $m = 10^2$ to $m = 10^5$, as observed by Liu et al. (2002), the unyielded zones, and particularly zone 1, change drastically with m. On the other hand, above this last value, there is no further influence of m and all the unyielded zones remain constant. This result is interesting particularly for zone 4 because its existence has been extensively discussed by Liu et al. (2002) and Zisis and Mitsoulis (2002). This analysis has been also carried out for other geometric configurations and shear thinning index (Deglo de Besses et al., 2003; Savreux et al., 2002), with the same result. Figure 6 shows that the increase with m of the drag coefficient C_d^* (defined below) is very weak above $m = 10^4$ (<0.05%). Thus the value $m = 3 \times 10^5$ has been used for all the calculations herein.

It has been also observed by the previous authors that the size of this zone 4 decreases with the mesh refinement. However, because this zone is very small and the reduction is very slow, it is difficult to give a definitive point of view on this question. So, for this zone and only for this one, it cannot be explicitly considered that there is convergence with the mesh refinement. Only an experimental approach could give a definitive response to the real existence of this zone. On the other hand, for the other rigid zones and for the drag coefficient, there is absolute convergence with the mesh refinement.

The size of these different zones depends to a great extent on

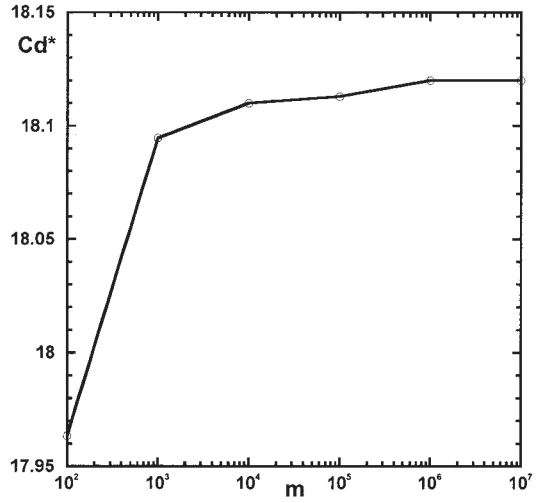

Figure 6. Influence of the regularization parameter *m* on the drag coefficient (Od = 0.5).

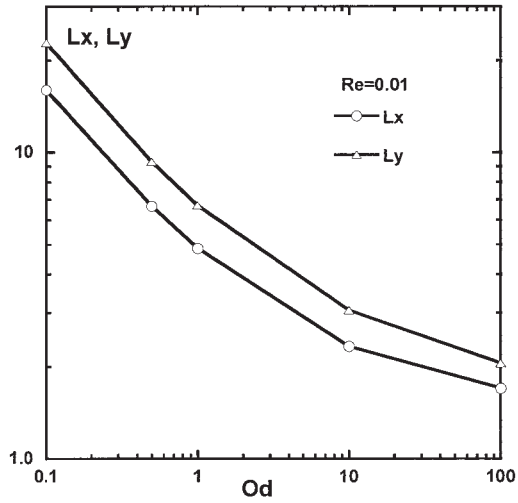

Figure 8. Influence of the Oldroyd number on the dimensions of the shear zone: Re = 0.01.

the dimensionless parameters (Od, Re). This point is examined in the following part.

Flows for negligible inertia

Figure 7 shows the change in the morphology of the flow when the Od number is increased up to 100. A general view and an enlarged view of the plate are presented. When the yield effect increases, the size of the sheared zone (the white region inside zone 1) substantially decreases. For a large Od number, this zone becomes very small, after which the region where the fluid flows becomes extremely reduced. Its dimensions *Lx*, *Ly* were measured (Figure 8). For Od = 100, *Lx* is scarcely equal to 2 times the length of the plate, whereas it was equal to more than 10 for Od = 0.1. Moreover, as can be seen in Figures 7 and 9, the dimensions *Lu* and *Ld* of the rigid static zones placed on either side of the plate (Figure 4: zones 2 and 3) also increase considerably with Od. This increase is particularly significant up to Od = 1 (Figure 9) and less pronounced >1. This overall increase in the rigid static zones with Od (or, in other words, the drastic reduction in the flow region) is not really surprising because as it has been shown in many other configurations (for example, Abdali and Mitsoulis, 1992), that for an infinite Od number, the unyielded regions should occupy all the domain. On the other hand, the rigid moving region (zone 4) seems to shrink and to move nearer to the plate with an increase in Od. This is attributed, as seen previously, to the localization of the flow between the plate with the two rigid static zones and zone 1, which produces an increase in the shear stresses and thus in the second invariant τ_{II}.

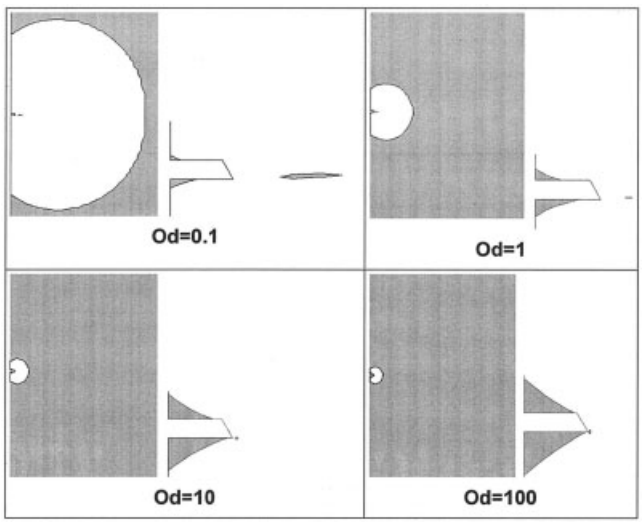

Figure 7. Influence of the Oldroyd number on unyielded zones: overall flow and zoom on the plate; inertia effect neglected.

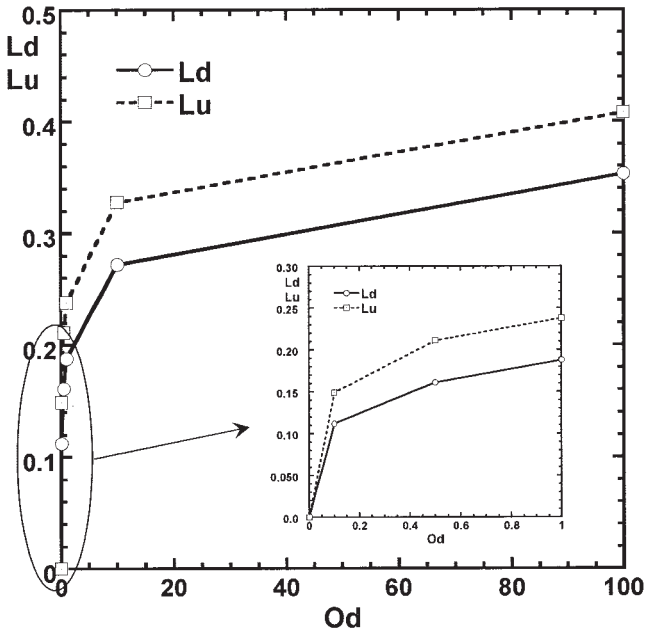

Figure 9. Influence of Od on the dimensions of the upstream rigid static zone (*Lu*) and on the downstream one (*Ld*): inertia effect neglected.

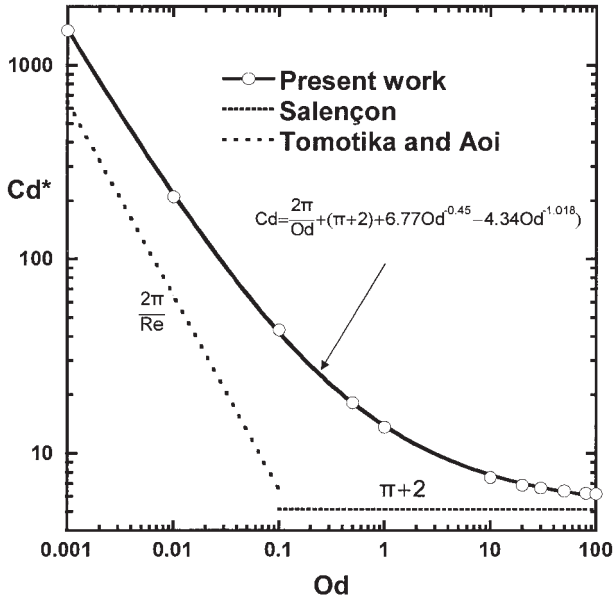

Figure 10. Influence of Od on the drag coefficient: inertia effect neglected.

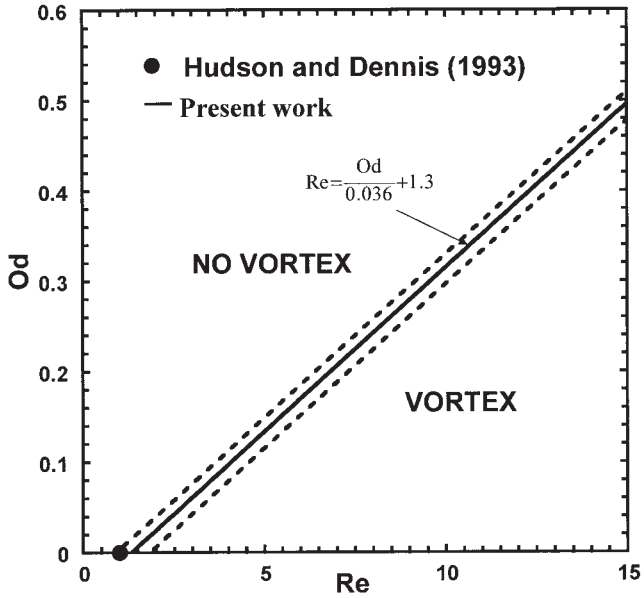

Figure 12. Map of vortex occurrence.

For a viscoplastic fluid, it is interesting to express the drag force as a sum of two terms, one corresponding to viscous effects and the other to yield effects

$$\frac{F_y}{l} = A \times (K \times U/l) + B \times \tau_0 \tag{11}$$

Thus a drag coefficient can be expressed in the following form, where A is a constant and B is a function of Od

$$C_{dv} = \frac{F_y/l}{(K \times U)/l} = A + B(\mathrm{Od}) \times \mathrm{Od} \tag{12}$$

C_d^* is defined by dividing this equation by the Oldroyd number

$$C_d^* = \frac{C_{dv}}{\mathrm{Od}} = \frac{A}{\mathrm{Od}} + B(\mathrm{Od}) \tag{13}$$

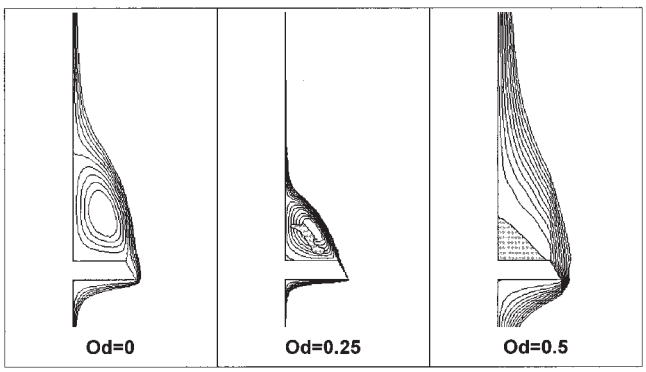

Figure 11. Change in flow structure around the plate in relation to Od: inertia effect neglected.

Figure 10 shows the influence of the Od number on C_d^*. This term decreases with increasing Od. After a fit of the calculated points, the following expression, which is valid for a negligible inertia and for Od tends to 0 (Newtonian case) to Od large, is proposed

$$C_d^* = \frac{2\pi}{\mathrm{Od}} + (\pi + 2) + (6.77\mathrm{Od}^{-0.45}) + (-4.34\mathrm{Od}^{-1.018}) \tag{14}$$

Two behaviors can be observed, for small and large yield stress numbers. For large Od numbers, the slope of the curve decreases dramatically and becomes very small for the largest values of Od. Salençon (1983) studied the cutoff of a half-space with a theoretical approach based on the Von Mises criterion and the limit analysis. He proposes a lower and upper limit for the force corresponding to an infinite Od number. The values calculated by Salençon are $5.0 \leq C_d^* \leq 5.47$. After a finer study this author proposes a value of $C_d^* = \pi + 2$. Thus in Eq. 14 when Od tends toward infinity, C_d^* tends to $\pi + 2$.

When the Od number is very small, the behavior of the fluid is close to that of a Newtonian one. However, according to the work of Tomotika and Aoi (1968) the viscous drag coefficient tends toward 2π. It can be noticed that the expression suggested by Eq. 14 overestimates the numerical values by a factor $< 3\%$.

Flows with inertia

Morphology of Flows. When inertia effects are greater than plastic ones, two vortices may appear behind the plate. The size of this vortex depends to a great extent on both the Re and Od numbers. For a small Re, the streamlines surround the plate without any vortex. The vortex appears for an Re number between 1 and 1.5 and its size increases dramatically thereafter with increasing Re. However, as soon as a yield stress effect is introduced, the vortex tends to disappear (Figure 11) and it is

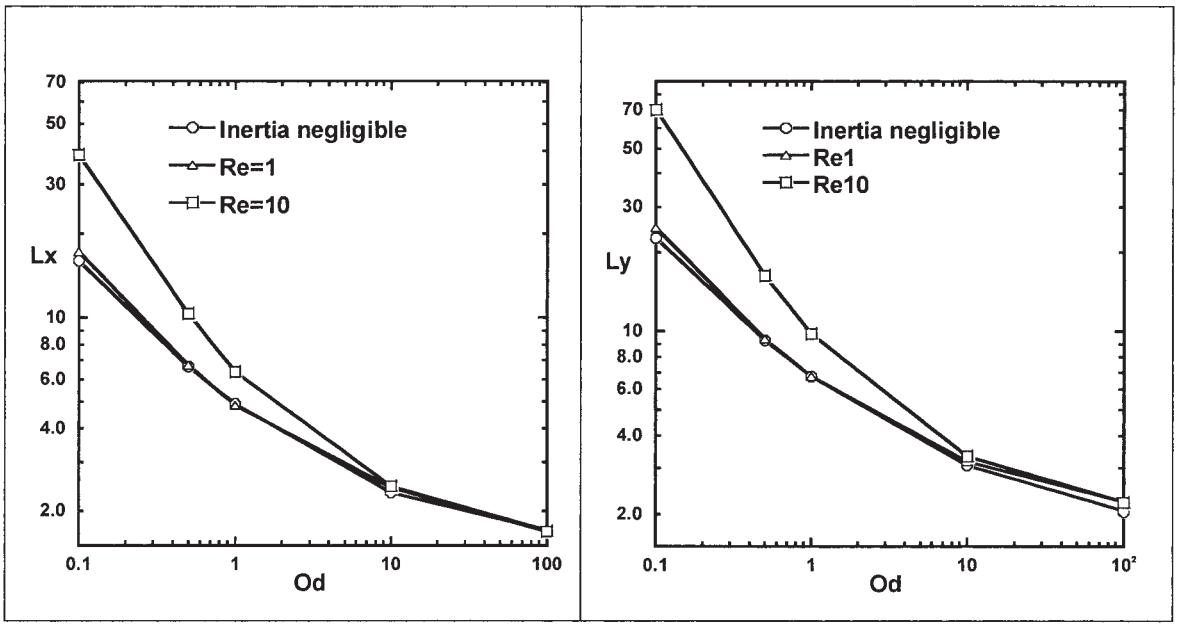

Figure 13. Influence of the Oldroyd number on the dimension of the shear zone for three Re numbers.

progressively replaced by the rigid static zone. In the case shown in Figure 11 (Re = 10), for Od = 0.25 a small unyielded zone appears in the middle of the plate (if one considers the entire plate) and another one inside the vortex. These two regions merge for Od = 0.5 and a rigid static zone is then created. It may be noticed that, for the case Od = 0.25, a rigid zone should appear at the break point between the vortex and the main flow. This zone must certainly be too small to be detected but it must exist.

From an industrial perspective, it is interesting to know whether there is a vortex depending on the Od and Re values. To solve this problem, a map of vortex occurrence is proposed (Figure 12). This map was obtained after a systematic analysis of the morphology of the flow. From this figure, it can be determined from which Re number there is a vortex for a given Od. It is not easy to determine the exact moment when the vortex appears because it is necessary to scan a very wide range of Re numbers for each Od. So an area of doubt is indicated instead of an exact value. From this figure it can be observed that the limit of occurrence of the vortex increases with the yield stress number. For an Od $>$ 1, the advent of a vortex should require a Reynolds number that is extremely large and certainly $>$50. The curve was fitted with a linear regression and the following equation was found

$$\mathrm{Re} = \frac{\mathrm{Od}}{0.036} + 1.3 \qquad (15)$$

Hudson and Dennis (1985) determined the streamlines behind the plate for $0.1 \leq \mathrm{Re} \leq 20$. A vortex can be observed on their figures from an Re value of 1, so this value has been added in Figure 12.

When the inertia effects are significant, the shear region is no longer centered on the middle of the plate, as observed for negligible Re (Figure 7), but is pushed slightly downstream. Moreover, this zone is much larger, especially for small Od numbers: *Lx* and *Ly* are almost multiplied by 2 between the cases Od = 0.1 Re negligible and Od = 0.1 Re = 10 (Figure 13). For large Od values, the yield effects are greater so the differences become less and these lengths are almost the same when inertia effects are neglected or not. For the rigid static zones (zones 2 and 3), when the Re number increases, the dimension of the downstream region (*Ld*, zone 2) increases, whereas that of the upstream one (*Lu*, zone 3) decreases. This effect can be particularly observed for Od numbers $<$ 20 (Figure 14). This point is interesting because it shows that the increase in inertia (such as in a process) does not eliminate the rigid static zones but modifies their configurations. Nevertheless, inertia seems to eliminate the rigid moving zones (zones

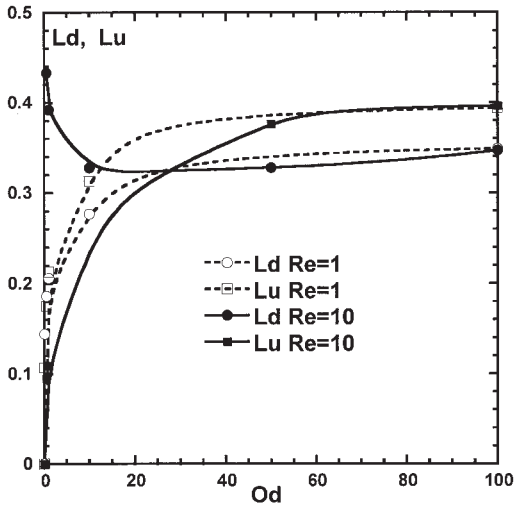

Figure 14. Influence of the Oldroyd number on the dimension of the rigid static zones.

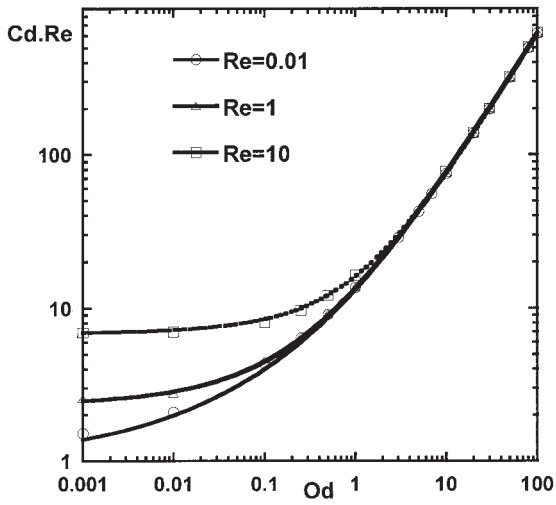

Figure 15. Influence of Od on (C_d× Re).

4) because in the case Re = 10 they have almost totally disappeared.

Drag Coefficient. Inertia obviously has a significant effect on the drag force, as seen in the section on Newtonian flows. When inertia acts, to obtain a pertinent drag coefficient, Eq. 10 must be divided by the inertia term ($\rho U^2 l$). Therefore, this relation takes the following form, where α is a constant and β is a function of Od

$$C_d \times \mathrm{Re} = \alpha + \beta(\mathrm{Od}) \times \mathrm{Od} \tag{16}$$

This term $C_d\times$ Re is plotted as a function of Od for three values of Re in Figure 15. When Od tends to zero (Newtonian case), the drag coefficient becomes constant and depends only on Reynolds number. Plasticity effects are negligible. The values can be estimated by Eqs. 10–12. For all Re, all curves merge when Od is sufficiently large. The plastic Reynolds number S becomes small. In this case, the flow can then be considered almost a creeping flow, and the behavior is the same as that for the case without inertia. When Re is negligible and Od large, the behavior is governed only by plasticity. The drag coefficient can be estimated by the asymptotic behavior of Eq. 17: $C_d = (\pi + 2)\mathrm{Od}$.

The following functions, which are valid for $0.001 \leq \mathrm{Od} \leq 100$, were found to describe the behaviors of various curves for the practical uses

For Re = 0.01

$$C_d \times \mathrm{Re} = 1.05 + (5.77 + 6.37\mathrm{Od}^{-0.57}) \times \mathrm{Od} \tag{17}$$

For Re = 1

$$C_d \times \mathrm{Re} = 2.34 + (5.51 + 5.57\mathrm{Od}^{-0.46}) \times \mathrm{Od} \tag{18}$$

For Re = 10

$$C_d \times \mathrm{Re} = 6.8 + (5.82 + 3.47\mathrm{Od}^{-0.5}) \times \mathrm{Od} \tag{19}$$

Conclusion

The flow normal to a flat plate of a Bingham fluid was studied numerically. The inertia effect was also considered.

When the inertia effect is very weak, the rigid stagnant zones placed on either side of the plate increase with the yield stress, whereas the shear zone around the plate decreases. The drag coefficient C_d^* decreases when the yield stress increases and seems to tend toward the asymptotic value $\pi + 2$ when the plasticity effects are predominant. This asymptotic value allows estimation of the stability of the plate.

When the inertia increases, a vortex appears downstream of the plate. A map showing the vortex occurrence, with respect to the Reynolds and the yield stress numbers, was proposed. The plasticity effects delay the advent of the vortex and reduce its size.

The results obtained on the size of the rigid zones and on the drag coefficient as functions of the plasticity and inertia effects are very useful to design processes such as viscoplastic fluid mixing.

Notation

C_d = drag coefficient, Eq. 9
C_d^* = drag coefficient, Eq. 13
D_{ij} = strain rate tensor
e = breadth of the plate
F_y = drag force per unit length
H = half breadth of the calculated domain
K = consistency factor
l = greatest length of the plate
L = length of the calculated domain
Lx = breadth of the shear flow zone
Ly = height of the shear flow zone
Lu = length of the upstream rigid static zone
Ld = length of the downstream rigid static zone
m = parameter of the Papanastasiou model
Od = Oldroyd number
Re = Reynolds number
S = plastic Reynolds number
U = fluid velocity

Greek letters

$\dot{\gamma}$ = second invariant of strain rate
τ_0 = yield stress
τ_{II} = second invariant of stress tensor deviator
τ_{ij} = stress tensor deviator
ρ = density

Literature Cited

Abdali, S. S., and E. Mitsoulis, "Entry and Exit Flows of Bingham Fluids," *J. Rheol.*, **36**, 389 (1992).

Acrivos, A., L. G. Leal, D. D. Snowden, and F. Pan, "Further Experiments on Steady Separated Flows Past Bluff Objects," *J. Fluid Mech.*, **34**, 25 (1968).

Alexandrou, A. N., E. Duc, and V. Entov, "Inertial, Viscous and Yield Stress Effects in Bingham Fluid Filling of a 2D Cavity," *J. Non-Newtonian Fluid Mech.*, **96**, 383 (2001).

Beris, A. N., J. A. Tsamopoulos, R. C. Armstrong, and R. A. Brown, "Creeping Motion of a Sphere through a Bingham Plastic," *J. Fluid Mech.*, **158**, 219 (1985).

Brookes, G. F., and R. L. Whitmore, "The Static Drag on Bodies in Bingham Plastics," *Rheol. Acta*, **7**, 189 (1968).

Brookes, G. F., and R. L. Whitmore, "Drag Forces on Bodies in Bingham Plastics," *Rheol. Acta*, **8**, 472 (1969).

Burgos, G. R., and A. N. Alexandrou, "Flow Development of Herschel–Bulkley Fluids in a Sudden Three Dimensional Square Expansion," *J. Rheol.*, **43**, 485 (1999).

Burgos, G. R., A. N. Alexandrou, and V. Entov, "On the Determination of Yield Surface in Herschel–Bulkley Fluids," *J. Rheol.*, **43**, 463 (1999).
Chabbra, R. P., *Bubbles, Drops and Particles in Non-Newtonian Fluids*, CRC Press, Boca Raton, FL (1993).
Deglo de Besses, B., A. Magnin, and P. Jay, "Viscoplastic Flow around a Cylinder in an Infinite Medium," *J. Non-Newtonian Fluid Mech.*, **115**(1), 27 (2003).
Dennis, S. C. R., Q. Wang, M. Coutanceau, and J.-L. Launay, "Viscous Flow Normal to a Flat Plate at Moderate Reynolds Numbers," *J. Fluid Mech.*, **248**, 605 (1993).
Hudson, J. D., and S. C. R. Dennis, "The Flow of a Viscous Incompressible Fluid Past a Normal Flat Plate at Low and Intermediate Reynolds Numbers: The Wake," *J. Fluid Mech.*, **160**, 369 (1985).
In, K. M., D. H. Choi, and M.-U. Kim, "Two-Dimensional Viscous Flow Past a Flat Plate," *Fluid Dyn. Res.*, **15**, 13 (1995).
Ingham, D. B., T. Tang, and B. R. Morton, "Steady Two-Dimensional Flow through a Row of Normal Flat Plates," *J. Fluid Mech.*, **210**, 281 (1990).
Jay, P., A. Magnin, and J. M. Piau, "Viscoplastic Fluid Flow through a Sudden Axisymmetric Expansion," *AIChE J.*, **47**, 2155 (2001).
Liu, B. T., S. J. Muller, and M. M. Denn, "Convergence of a Regularisation Method for Creeping Flow of a Bingham Material about a Rigid Sphere," *J. Non-Newtonian Fluid Mech.*, **102**, 179 (2002).
Papanastasiou, T. C., "Flow Material with Yield," *J. Rheol.*, **31**, 385 (1987).
Pazwash, H., and J. M. Robertson, "Forces on Bodies in Bingham Fluids," *J. Hydrol. Res.*, **13** (1975).
Piau, J. M., "Viscoplastic Boundary Layer," *J. Non-Newtonian Fluid Mech.*, **102**, 193 (2002).
Salençon, J., *Cours de calcul des structures anélastiques, calcul à la rupture et analyse limite*, Presses de l'Ecole Nationale des Ponts et Chaussées, Paris (1983).
Savreux, F., P. Jay, and A. Magnin, "Structure of Flows in Viscoplastic Fluid Mixing," Proc. of ASME "FEDSM 2002," Montreal, Canada (2002).
Smyrnaios, D. N., and J. A. Tsamopoulos, "Squeeze Flow of Bingham Plastics," *J. Non-Newtonian Fluid Mech.*, **100**, 165 (2001).
Tamada, K., H. Miura, and T. Miyagi, "Low-Reynolds-Number Flow Past a Cylindrical Body," *J. Fluid Mech.*, **132**, 445 (1983).
Tanner, R. I., "Stokes Paradox for Power-Law Flow around a Cylinder," *J. Non-Newtonian Fluid Mech.*, **50**, 217 (1993).
Tomotika, S., and T. Aoi, "The Steady Flow of a Viscous Fluid Past an Elliptic Cylinder and a Flat Plate at Small Reynolds Numbers," *Q. J. Mech. Appl. Math.*, **6**, 290 (1952).
Wu, J., and M. C. Thompson, "Non Newtonian Shear-Thinning Flows Past a Flat Plate," *J. Non-Newtonian Fluid Mech.*, **66**, 127 (1996).
Zisis, Th., and E. Mitsoulis, "Viscoplastic Flow around a Cylinder Kept between Parallel Plates," *J. Non-Newtonian Fluid Mech.*, **105**, 1 (2002).

Manuscript received Aug. 26, 2003, and revision received July 13, 2004.